BLIND SEPARATION OF COMPLEX-VALUED MIXTURES: SPARSE REPRESENTATION IN POLAR AND CARTESIAN SCATTER-PLOTS

Ehud Orian, Yehoshua Y. Zeevi

Technion—Israel Institute of Technology
Department of Electrical Engineering
Haifa 32000, Israel
Emails: oriane@tx.technion.ac.il , zeevi@ee.technion.ac.il

ABSTRACT

This study is concerned with reconstruction of complex-valued components comprising a linear mixing model of unknown real-valued sources, given a set of their complex-valued mixtures. We adopt previous results in the area of Blind Source Separation (BSS) of linear mixtures, based on sparse representation by means of a multiscale framework such as wavelet packets, and exploit the properties of sparse representation obtained by projection onto a proper space. We propose two techniques, developed for dealing with complex-valued mixtures of real sources and incorporate sparsity-dependent clustering via projection onto a proper space; one onto polar coordinates, and the other onto cartesian coordinates. We describe various aspects of the proposed techniques, and present an experiment of noisy mixtures of images.

Keywords: Blind Source Separation, Complex-Valued Mixtures, Sparse Representation, Multiscale Transforms, Wavelet Packets.

1. INTRODUCTION

Blind separation of mixtures of images is an essential processing technique, required in various practical applications, e.g. separation of an image from reflections superimposed by semireflections [1]. In some applications such as MRI and Radar, the mixtures are complex although the sources are real. Thus, in such cases, given N linear mixtures of M signals or images:

$$\mathbf{x}(k) = \mathbf{A}\mathbf{s}(k) + \mathbf{n}(k) \quad k = 1, 2, \ldots, \tag{1}$$

where $\mathbf{x}(k)$ and $\mathbf{n}(k)$ are $N \times 1$ complex vectors, $\mathbf{s}(k)$ is $M \times 1$ real vector and $\mathbf{A}$ is a $N \times M$ complex matrix consists of unknown values and $N \geq M$. The unknown components $s_i(k)$ of $\mathbf{s}(k)$, referred to as 'sources', are usually assumed to be statistically and independent [2]. This assumption can, according to the approach adopted in this paper, be relaxed. The observed 'mixtures' $x_i(k)$, are possibly corrupted by additive noise $\mathbf{n}(k)$. The independent variable k represents in our case spatial coordinate(s).

The common approach to solving the inverse problem (i.e. sources recovery) is based on estimation of the mixing matrix $\mathbf{A}$ or, equivalently, its inverse matrix $\mathbf{W}$ which yields the best estimate of the sources by means of its product with the mixtures:

$$\hat{\mathbf{s}}(k) = \hat{\mathbf{W}}\mathbf{x}(k) \quad k = 1, 2, \ldots. \tag{2}$$

Several approaches have been suggested for this purpose (see for example [3, 4, 5]). Note that the recovery of the mixing matrix is up to column permutation and scaling (or equivalently sources permutation and scaling), since these operations can be interchanged between the unknown sources and the matrix.

The main objective of this paper is to advance a processing technique, suitable for separation of complex-valued mixtures of real sources. We address, however, also the problem wherein the sources are complex as well.

This research has been supported by the HASSIP Research Network Program, sponsored by the European Commission and by the Ollendorff Minerva Center for Vision and Image Sciences.

2. PRELIMINARIES

Whereas the histograms of gray levels of natural image sources or mixtures are broadly distributed, indicating that images are highly correlated, projection onto a sparse space of representation decorrelates the images and, consequently, the pdf of a projected source (or mixture) coefficients decays rapidly. Thus, thresholding the values of the coefficients of the transformed signals yields sparse representations. Indeed, the probability of a coincidence of the transformed images approaches zero, since the cross-correlation is practically zero. This sparse representation permits a simple geometric estimation of the mixing matrix [3]. Let us use the basis of decomposition functions, $\{\varphi_\gamma(k)\}_{\gamma\in\Omega}$, in the representation of the real sources $\{\mathbf{s}_m(k)\}_{m=1}^{M}$:

$$\mathbf{s}_m(k) = \sum_{\gamma\in\Omega} c_{m\gamma}\varphi_\gamma(k) \quad k = 1, \ldots, M, \tag{3}$$

where the functions (features) $\varphi_\gamma(k)$, called atoms or elements of the representation space, represent each source $\mathbf{s}_m$ by its corresponding real-valued decomposition coefficients $c_{m\gamma}$. Sparsity, can therefore be expressed as an appropriate representation such that for each source $\mathbf{s}_m$ there exists a subset $G_m \subset \Omega$, corresponding to the function set $\{\varphi_\gamma(k)\}_{\gamma\in G_m}$ where:

$$|c_{m\gamma}| \gg |c_{n\gamma}| \quad \forall\gamma \in G_m, \quad m \neq n. \tag{4}$$

Separation performance strongly depends on sparseness properties of the representation, such as the relative sizes of the sparse sets, i.e. $|G_m|/|\Omega|$, the ratios $|c_{m\gamma}|/|c_{n\gamma}|$ when $\gamma \in G_m$, $m \neq n$ and the ratios $|c_{m\gamma}|/|c_{m\rho}|$ when $\gamma \in G_m$, $\rho \notin G_m$.

3. THE PROPOSED TECHNIQUES

3.1 Sparse Scatter Plots in Polar Coordinates

The complex mixing matrix in polar coordinates is:

$$\mathbf{A} = \begin{pmatrix} a_{11} & \ldots & a_{1M} \\ \vdots & \ddots & \vdots \\ a_{N1} & \ldots & a_{NM} \end{pmatrix} = \begin{pmatrix} r_{11}e^{j\theta_{11}} & \ldots & r_{1M}e^{j\theta_{1M}} \\ \vdots & \ddots & \vdots \\ r_{N1}e^{j\theta_{N1}} & \ldots & r_{NM}e^{j\theta_{NM}} \end{pmatrix}$$

$$r_{ij} > 0,\, \theta_{ij} \in [0\,2\pi], \tag{5}$$

where θ_{ij} as well as r_{ij} are unknown. We apply a transformation (3) that yields a highly-sparse representation:

$$\tilde{\mathbf{x}}(\gamma) = \mathbf{A}\tilde{\mathbf{s}}(\gamma) + \tilde{\mathbf{n}}(\gamma) \quad \gamma = 1, 2, \ldots, \tag{6}$$

where the m-th element of $\tilde{\mathbf{s}}(\gamma)$ is the decomposition coefficient of the source $\mathbf{s}_m(k)$, corresponding to the representation function $\varphi_\gamma(k)$:

$$\tilde{\mathbf{s}}(\gamma) = \begin{pmatrix} c_{1\gamma} \\ \vdots \\ c_{M\gamma} \end{pmatrix}. \tag{7}$$

Since it is a sparse representation, for each source $\mathbf{s}_m$ there exists a group G_m where:

$$|c_{m\gamma}| \gg |c_{n\gamma}| \quad \forall n \neq m, \gamma \in G_m\,, \tag{8}$$

i.e. only one coefficient of $\tilde{\mathbf{s}}(\gamma)$ is dominant.

By using (6),(7),(8), and taking the absolute values (element-wise) of the transformed mixtures $\tilde{\mathbf{x}}(\gamma)$, we obtain:

$$\begin{aligned}
|\tilde{\mathbf{x}}(\gamma)|^\bullet &\triangleq \begin{pmatrix} |\tilde{\mathbf{x}}_1(\gamma)| \\ \vdots \\ |\tilde{\mathbf{x}}_N(\gamma)| \end{pmatrix} \\
&\approx \begin{pmatrix} \left| c_{m_0\gamma} r_{1m_0} e^{j\theta_{1m_0}} + \sum\limits_{m\neq m_0}^{M} c_{m\gamma} r_{1m} e^{j\theta_{1m}} \right| \\ \vdots \\ \left| c_{m_0\gamma} r_{Nm_0} e^{j\theta_{Nm_0}} + \sum\limits_{m\neq m_0}^{M} c_{m\gamma} r_{Nm} e^{j\theta_{Nm}} \right| \end{pmatrix} \\
&\approx \begin{pmatrix} \left| c_{m_0\gamma} r_{1m_0} e^{j\theta_{1m_0}} \right| \\ \vdots \\ \left| c_{m_0\gamma} r_{Nm_0} e^{j\theta_{Nm_0}} \right| \end{pmatrix} = \begin{pmatrix} \left| c_{m_0\gamma} r_{1m_0} \right| \\ \vdots \\ \left| c_{m_0\gamma} r_{Nm_0} \right| \end{pmatrix} \\
&= \left| c_{m_0\gamma} \right| \begin{pmatrix} r_{1m_0} \\ \vdots \\ r_{Nm_0} \end{pmatrix}, \quad \gamma \in G_{m_0}\,,
\end{aligned} \tag{9}$$

where the first approximation disregards the noise effect and the second approximation is justified for high sparsity related to the subscript γ. From (9) we infer that the scatter of the absolutes' vector $|\tilde{\mathbf{x}}(\gamma)|^\bullet$ is clustered around large values, along the orientation corresponding to the m_0-th column of the matrix $|\mathbf{A}|^\bullet$ (element-wise 'absolute matrix' of the complex mixing matrix $\mathbf{A}$). When there is absolutely no knowledge about the subsets $\{G_m\}_{m=1}^M$, we perform the absolutes' scatter-plot for all the subscripts $\{\gamma : \gamma \subset \Omega\}$ on the same coordinate system of the absolute-values' space. This results in clustering along M orientations, corresponding to the columns of $|\mathbf{A}|^\bullet$, as is demonstrated in Fig. 1.

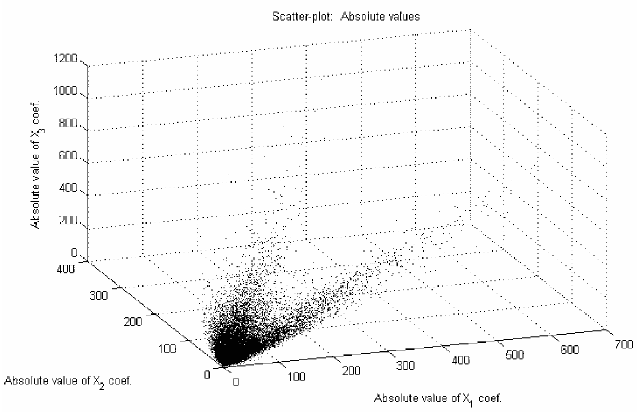

Figure 1: Scatter plot in absolute-values' space. $M = 2, N = 3$.

If the orientations corresponding to columns of $|\mathbf{A}|^\bullet$ are sufficiently spaced apart in the sense of not being collinear or wrapped by the previous approximations, then the orientations are distinguishable and a clustering algorithm can be performed to extract the orientations of the absolutes. Each additional (and-not-ill) observed mixture contributes to the distinguishing ability by adding dimension to the absolute-values' space.

A similar view holds for the element-wise argument of $\tilde{\mathbf{x}}(\gamma)$:

$$\begin{aligned}
\arg\{\tilde{\mathbf{x}}(\gamma)\}^\bullet &\triangleq \begin{pmatrix} \arg\{\tilde{\mathbf{x}}_1(\gamma)\} \\ \vdots \\ \arg\{\tilde{\mathbf{x}}_N(\gamma)\} \end{pmatrix} \\
&\approx \begin{pmatrix} \arg\left\{ c_{m_0\gamma} r_{1m_0} e^{j\theta_{1m_0}} + \sum\limits_{m\neq m_0}^{M} c_{m\gamma} r_{1m} e^{j\theta_{1m}} \right\} \\ \vdots \\ \arg\left\{ c_{m_0\gamma} r_{Nm_0} e^{j\theta_{Nm_0}} + \sum\limits_{m\neq m_0}^{M} c_{m\gamma} r_{Nm} e^{j\theta_{Nm}} \right\} \end{pmatrix} \\
&\approx \begin{pmatrix} \arg\left\{ c_{m_0\gamma} r_{1m_0} e^{j\theta_{1m_0}} \right\} \\ \vdots \\ \arg\left\{ c_{m_0\gamma} r_{Nm_0} e^{j\theta_{Nm_0}} \right\} \end{pmatrix} \\
&= \arg\{c_{m_0\gamma}\} + \begin{pmatrix} \theta_{1m_0} \\ \vdots \\ \theta_{Nm_0} \end{pmatrix}, \quad \gamma \in G_{m_0}\,.
\end{aligned} \tag{10}$$

Therefore, the scatter of $\arg\{\tilde{\mathbf{x}}(\gamma)\}^\bullet$ is clustered around the point which corresponds to the m_0-th column of the matrix $\arg\{\mathbf{A}\}^\bullet$ (element-wise argument of the complex mixing matrix $\mathbf{A}$) and its π shifted bonus (since $c_{m\gamma}$ are real, $\arg\{c_{m\gamma}\} = 0$ or π). An important matter is that by performing the argument scattering of each absolute-orientation scatter subset, previously clustered, in a different coordinate system, we can ascribe each argument-vector to its absolute-orientation. This prevents uncertainty in assignment of each argument-vector to its absolute-orientation.

3.1.1 Sparsity Dependent Clustering

Since the approximations in (9) and (10) are justified for high sparsity related to the subscript γ, the clustering should be sparsity-dependent. In this case, high sparsity of scatter points is related to their vicinity to the estimated orientation and magnitude of their projection onto orientational cluster. Therefore a suitable sparsity consideration should be applied in order to extract the absolute orientations and their argument-vectors. One possibility for such a consideration is to examine the histogram of orientations in the scatter space of $|\tilde{\mathbf{x}}(\gamma)|^\bullet$ (demonstrated in Fig. 4) and then extract its M centers. The scatter points which are related to each center can then be taken for extraction of their center argument-vectors.

3.1.2 Image Source Recovery

The meaning of the argument-vector estimation uncertainty mod(π), is that the estimation of each complex column vector of the mixing matrix $\mathbf{A}$, $(r_{1m}e^{j\theta_{1m}}, \ldots, r_{Nm}e^{j\theta_{Nm}})^T$ is up to switching with its opposite vector, i.e. $(-r_{1m}e^{j\theta_{1m}}, \ldots, -r_{Nm}e^{j\theta_{Nm}})^T$. This is equivalent to switching the sign of the m-th source. In addition, each absolute-vector estimation is up to positive scaling and lacks the ascription to column-positioning in the mixing matrix $\mathbf{A}$. Therefore, the union of the above claims withstands the fact that the recovery is up to permutation and scaling.

The estimated mixing matrix $\hat{\mathbf{A}}$ is obtained by assigning each estimated absolute-vector $(\hat{r}_{1m}, \ldots, \hat{r}_{Nm})^T$ to its estimated argument-vector $(\hat{\theta}_{1m}, \ldots, \hat{\theta}_{Nm})^T$:

$$(\hat{a}_{1m}, \ldots, \hat{a}_{Nm})^T = (\hat{r}_{1m}e^{j\hat{\theta}_{1m}}, \ldots, \hat{r}_{Nm}e^{j\hat{\theta}_{Nm}})^T\,. \tag{11}$$

We then use the Matlab's matrix left division (Pseudo Inverse) to recover the sources from the observed mixtures, i.e.:

$$\hat{\mathbf{s}}(k) = \hat{\mathbf{A}} \backslash X(k) \quad k = 1, 2, \ldots \quad . \tag{12}$$

3.2 Sparse Scatter Plots in Cartesian Coordinates

The complex mixing matrix in cartesian (real-imaginary) coordinates is:

$$\mathbf{A} = \begin{pmatrix} a_{11} & \dots & a_{1M} \\ \vdots & \ddots & \vdots \\ a_{N1} & \dots & a_{NM} \end{pmatrix} = \begin{pmatrix} \alpha_{11}+j\beta_{11} & \dots & \alpha_{1M}+j\beta_{1M} \\ \vdots & \ddots & \vdots \\ \alpha_{N1}+j\beta_{N1} & \dots & \alpha_{N1}+j\beta_{NM} \end{pmatrix}$$

$$\alpha_{ij}, \beta_{ij} \in \mathbb{R}, \qquad (13)$$

where α_{ij} as well as β_{ij} are unknown and i.i.d. As in section 3.1, we applied a transformation (3) that yields a highly-sparse representation. Since the sources are real, each of their complex mixtures is equivalent to a pair of (independent) mixtures, corresponding to the real and imaginary parts of (1). Technically, we perform directions clustering for separated scatter-plots of the mixtures' real and imaginary parts (as demonstrated in Fig. 2), thus recovering the matrixes $\mathrm{Re}(\mathbf{A})$ and $\mathrm{Im}(\mathbf{A})$ up to column permutation and scaling. Recovering the complex matrix $\mathbf{A}$ (still up to column permutation

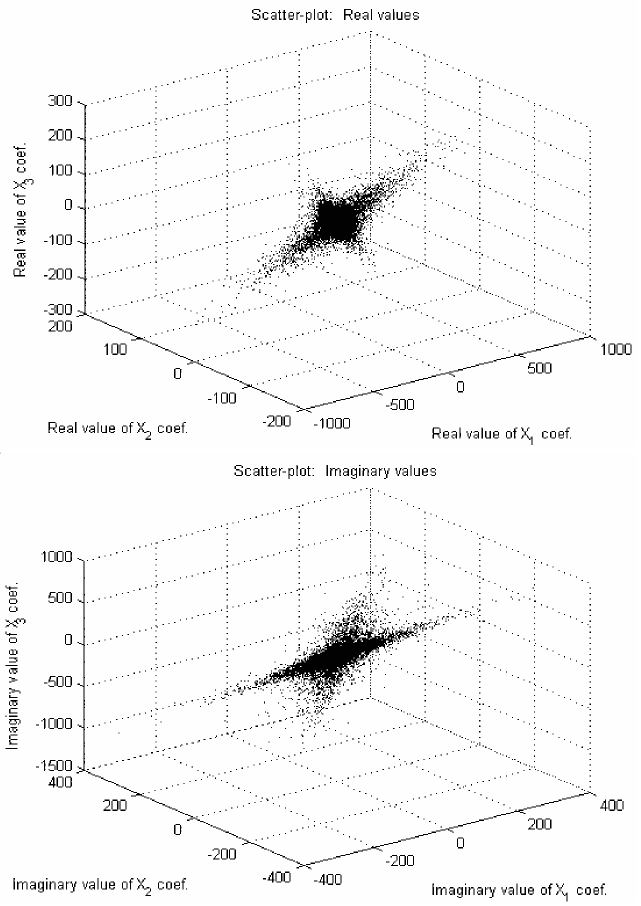

Figure 2: Scatter-plots of the mixtures' real and imaginary parts. $M = 2, N = 3$.

and scaling) requires assignment of each real column to its correct scaled imaginary column, so at first glance, those uncertainties seem to be devastating. However, it can be easily solved since we can exactly ascribe the real and imaginary data points to each other, this enables tracing the correct assignment and scaling of real and imaginary columns, as can be induced from Fig. 3 which describes the cartesian (Real/Imaginary) scatter points of high-sparsity related to a subscript γ by presenting the case of $c_{n\gamma} = 0$, $c_{m\gamma} \neq 0$, $\forall n \neq m$ $\gamma \in G_m$.

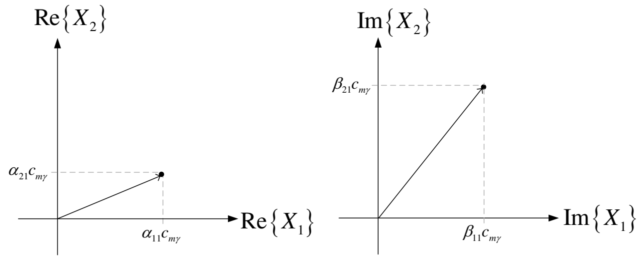

Figure 3: Cartesian (Real/Imaginary) scatter points of high-sparsity related to a subscript γ in the case of $c_{n\gamma} = 0$, $c_{m\gamma} \neq 0$, $\forall n \neq m$, $\gamma \in G_m$. $N = 2$.

4. EXPERIMENTAL RESULTS

We demonstrate the technique of scatter-plots in polar coordinates (Section 3.1) through image-sources. Three synthetic complex-valued mixtures of 'Blond' and 'Brunette', corrupted by i.i.d complex-valued noise of 25dB S/N, are used in our separation process. The absolute-value images of two of the three complex-valued mixtures are depicted in Fig. 4.

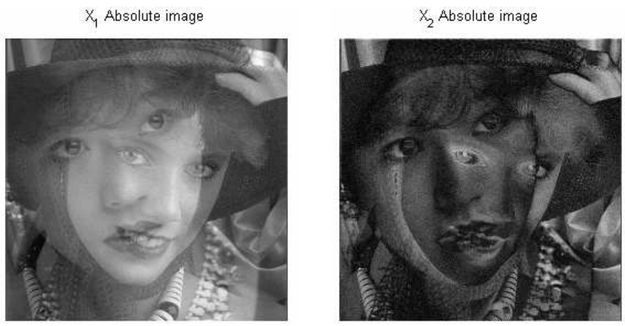

Figure 4: Absolute-value images of two of the three complex-valued mixtures (size: 256×256).

Two-dimensional wavelet packet decomposition is performed, using node (2,1) of the 5th-order Coifman Wavelets. Scatter points of low norm (comprising the dark area in Fig. 6) are neglected and the rest of the scatter points (about 30%) are taken to form a histogram of orientations in the absolute-values' scatter space. The histogram is then smoothed to extract the absolute-directions from both its centers, as shown in Fig. 5.

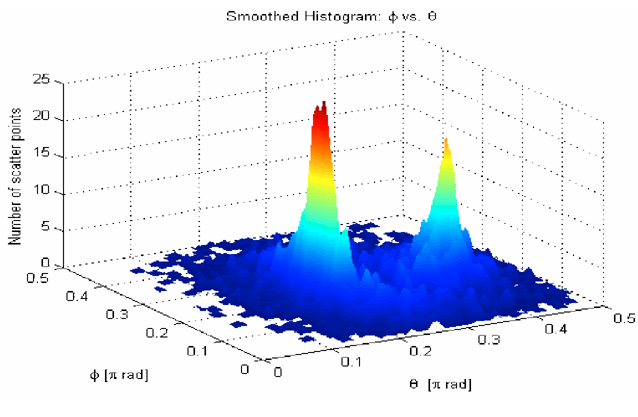

Figure 5: Orientational histogram of scatter points in the absolute-values' scatter space.

Thus, an estimation of the true absolute-orientations can be made, as shown in Fig. 6.

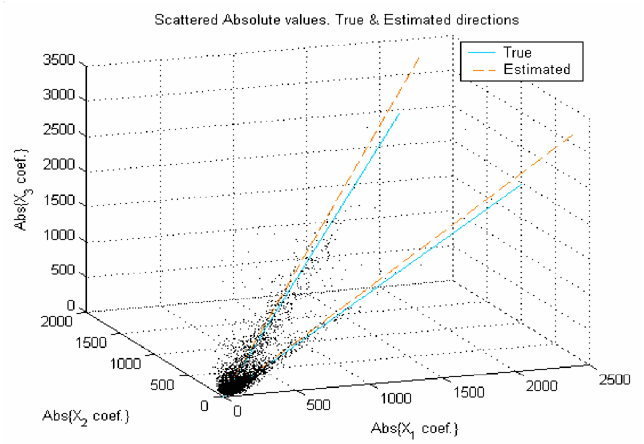

Figure 6: Absolute values' scatter plot. The true orientations (solid) and the estimated ones (dashed).

The arguments of scatter points which are highly related to the estimated orientations (about 0.07% of total) are then taken in order to extract the estimated argument-vectors from their centers in the argument-values' Half-space (i.e. accounting for mod(π)), as shown in Fig. 7.

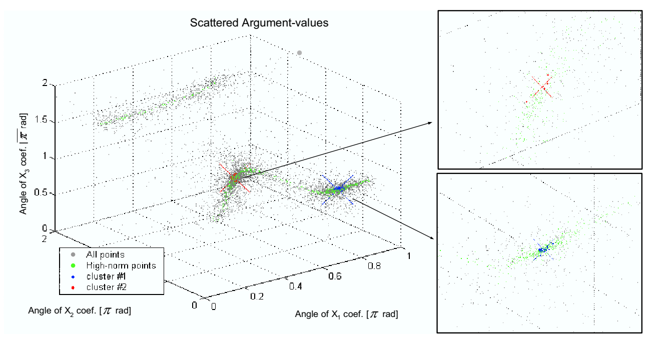

Figure 7: Argument-values Half-space scatter-plot. Clustered values are marked with a cross. Both concentrations are zoomed to the right.

Assigning each argument-vector to its absolute-orientation is equivalent to recovering the columns of the complex mixing matrix (up to permutation and scaling). Using pseudo inverse, the source images are then recovered as well. Taking the absolute values of their real part, and presenting the grayscale intensity of each recovered source within its data range, scaling uncertainty becomes less significant. Finally, de-noising filtering can be performed using any knowledge of the sources and noise. In this example we performed a low pass filtering. The recovered images, compared to their origins, are presented in Fig. 8. A noise-free similar experiment, results in estimated sources indistinguishable from their originals. Results obtained with the noisy data can be improved by adaptive selection of data subsets from different nodes.

5. DISCUSSION AND CONCLUSIONS

Sparse representation of complex-valued mixtures of images in polar coordinates facilitates the development of new and efficient algorithms for blind separation of image sources. Although the major goal of this study is the application of our techniques to blind separation of tissues using a set of MR images [7], we are mostly using

Figure 8: Recovered images (under 25 db S/N) compared to their origins.

synthetic mixtures, where the ground truth is available. Based on our experiments with such synthetic images we may conclude that the proposed technique can also be applied to volumetric images data and/or higher dimensional representations of images.

REFERENCES

[1] M. Bronstein, A. Bronstein, M. Zibulevsky and Y.Y. Zeevi, "Separation of Reflections via Sparse ICA," *ICIP*, Vol. 4, pp. 313–316, 2003.

[2] J.F Cardoso, "Performance and Implementation of Invariant Source Separation Algorithms," *ISCAS'96*, 1996.

[3] P. Kisilev, M. Zibulevsky, and Y.Y. Zeevi, "A Multiscale Framework For Blind Source Separation," *Journal of Machine Learning Research*, Vol. 4, pp. 1339–1363, 2003.

[4] A.M. Bronstein, M.M. Bronstein, M. Zibulevsky and Y.Y. Zeevi, ""Unmixing" Tissues: Sparse Component Analysis in Multi-Contrast MRI", submitted to *ICIP 2005*.

[5] J.F Cardoso and Beate Laheld, "Equivariant Adaptive Source Separation," *IEEE Trans.*, Vol. 44, No. 12, pp. 3017–3030, 1996.

[6] S.C. Chen, D.L. Donoho and M.A. Sanders, "Atomic Decomposition by Basis Pursuit," *SIAM Review*, Vol. 43, No. 1, pp. 129–159, 2001.

[7] W. Thomas Dixon, "Simple Proton Spectroscopic Imaging," *Radiology*, Vol. 153, pp. 189–194, 1984.